Neuron
Article

ELKS2α/CAST Deletion Selectively Increases Neurotransmitter Release at Inhibitory Synapses

Pascal S. Kaeser,[1,3,7] Lunbin Deng,[1,3,7] Andrés E. Chávez,[6] Xinran Liu,[3] Pablo E. Castillo,[6] and Thomas C. Südhof[1,2,3,4,5,*]
[1]Department of Molecular and Cellular Physiology
[2]Howard Hughes Medical Institute
Stanford University School of Medicine, 1050 Arastradero Road, Palo Alto, CA 94304-5543, USA
[3]Department of Neuroscience
[4]Department of Molecular Genetics
[5]Howard Hughes Medical Institute
The University of Texas Southwestern Medical Center, Dallas, TX 75390-9111, USA
[6]Dominick P. Purpura Department of Neuroscience, Albert Einstein College of Medicine, Bronx, NY 10461, USA
[7]These authors contributed equally to this work
*Correspondence: tcs1@stanford.edu
DOI 10.1016/j.neuron.2009.09.019

SUMMARY

The presynaptic active zone is composed of a protein network that contains ELKS2α (a.k.a. CAST) as a central component. Here we demonstrate that in mice, deletion of ELKS2α caused a large increase in inhibitory, but not excitatory, neurotransmitter release, and potentiated the size, but not the properties, of the readily-releasable pool of vesicles at inhibitory synapses. Quantitative electron microscopy revealed that the ELKS2α deletion did not change the number of docked vesicles or other ultrastructural parameters of synapses, except for a small decrease in synaptic vesicle numbers. The ELKS2α deletion did, however, alter the excitatory/inhibitory balance and exploratory behaviors, possibly as a result of the increased synaptic inhibition. Thus, as opposed to previous studies indicating that ELKS2α is essential for mediating neurotransmitter release, our results suggest that ELKS2α normally restricts release and limits the size of the readily-releasable pool of synaptic vesicles at the active zone of inhibitory synapses.

INTRODUCTION

Active zones are specialized parts of the presynaptic plasma membrane where synaptic vesicles dock and fuse to release their neurotransmitter content into the synaptic cleft (Schoch and Gundelfinger, 2006; Südhof, 2004). Active zones are composed of a large protein complex containing members of at least five protein families: Munc13s, RIMs, piccolo/bassoon, α-liprins, and ELKS (Figure 1A). Of these proteins, RIMs and ELKS are biochemically central elements because they bind to each other and to all other active zone proteins (Ohtsuka et al., 2002; Takao-Rikitsu et al., 2004; Wang et al., 2002).

Analyses of mouse, *Drosophila*, and *C. elegans* mutants have suggested that the various active zone proteins, despite being part of the same protein complex, perform distinct functions in release. Specifically, both Munc13s and RIMs are required for synaptic vesicle priming (Aravamudan et al., 1999; Augustin et al., 1999; Calakos et al., 2004; Castillo et al., 2002; Junge et al., 2004; Kaeser et al., 2008; Koushika et al., 2001; Rhee et al., 2002; Richmond et al., 1999; Rosenmund et al., 2002; Schoch et al., 2002; Varoqueaux et al., 2002). Munc13s and RIMs additionally mediate use-dependent changes of neurotransmitter release, i.e., presynaptic plasticity, but are selectively essential for distinct forms of presynaptic plasticity. Munc13s are required for augmentation and related types of short-term plasticity (Rhee et al., 2002; Rosenmund et al., 2002), whereas RIMs are required for paired-pulse facilitation/depression and various types of presynaptic long-term plasticity (Calakos et al., 2004; Castillo et al., 2002; Chevaleyre et al., 2007; Schoch et al., 2002). Much less is known about α-liprins and piccolo/bassoon. In invertebrates, α-liprins are essential for maintaining the normal active zone structure as viewed by electron microscopy (Kaufmann et al., 2002; Patel et al., 2006; Serra-Pages et al., 1998; Zhen and Jin, 1999), but their role has not been examined physiologically, and their function in vertebrate nerve terminals has not been studied. Unlike other active zone proteins, bassoon and piccolo are not evolutionarily conserved. Deletion of bassoon partially silences synapses (Altrock et al., 2003), but its molecular role or that of piccolo remains largely unclear.

ELKS (also known as Rab6-interacting protein, CAST, and ERC; see references cited below) is a recently described, evolutionarily conserved active zone component that has been associated with many diverse functions. ELKS1 was identified as a gene fusion partner with the receptor tyrosine kinase RET in leukemia, and was named ELKS1 because of its high content in glutamic acid (E), leucine (L), lysine (K), and serine (S) (Nakata et al., 1999). ELKS1 was later characterized as a trans-Golgi Rab6-interacting protein (Monier et al., 2002), whereas ELKS2 (also named CAST or ERC1) was reported as an active zone protein (Ohtsuka et al., 2002; Wang et al., 2002). Vertebrates express two *ELKS* genes (*ELKS1* and *ELKS2*; note that in the CAST nomenclature ELKS1 = CAST2, and vice versa, whereas in the ERC nomenclature ELKS1 = ERC1 and vice

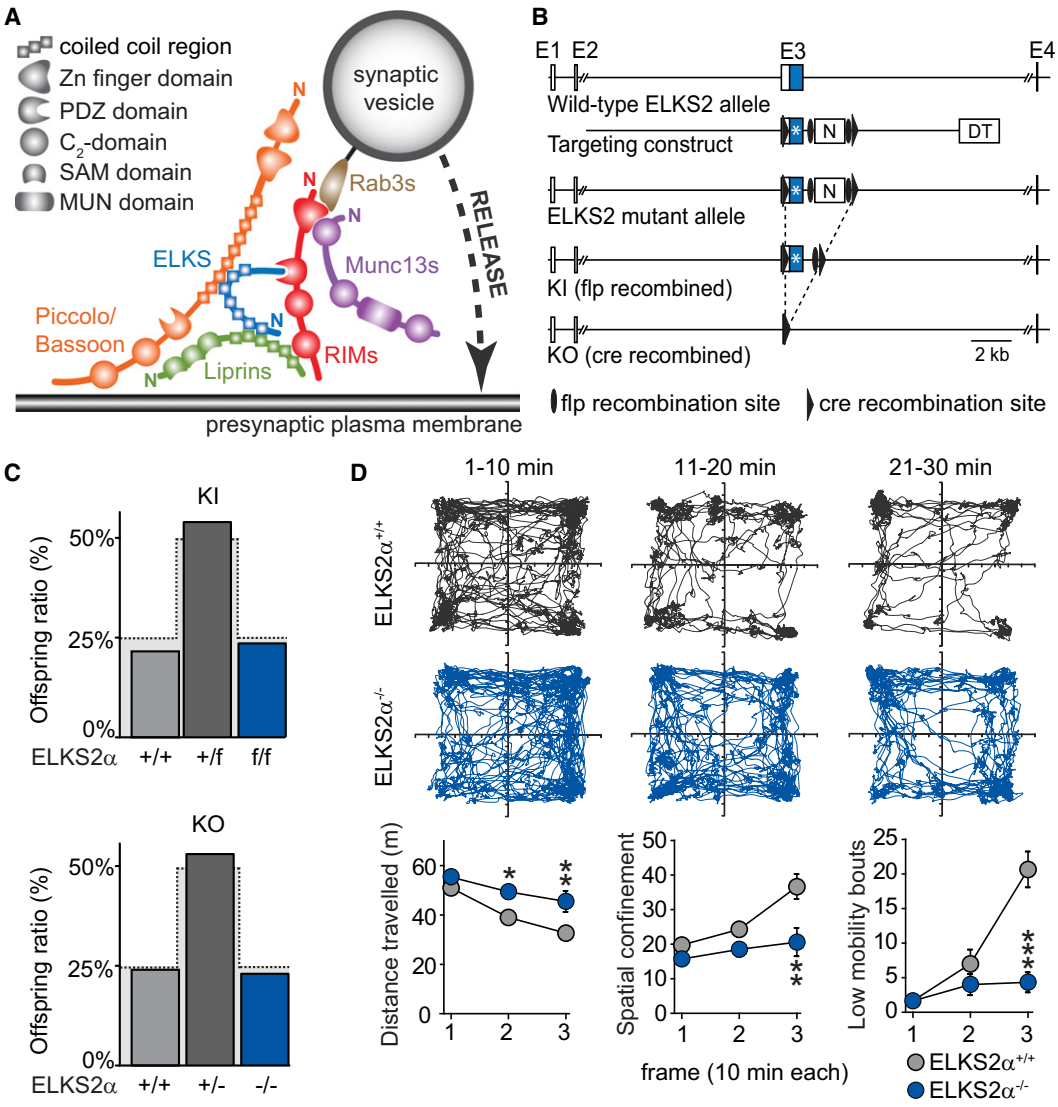

Figure 1. Generation of the ELKS2α Mutant Mice

(A) Schematic representation of the active zone protein complex containing RIMs and ELKS as central components that connect to synaptic vesicles and to all other active-zone proteins.

(B) Targeting strategy for the ELKS2 gene, showing (from top to bottom) the ELKS2 gene, a map of the targeting vector, the mutant allele of the founder line, the flp recombined KI allele, and the cre recombined KO allele. N, neomycin resistance cassette; DT, diphtheria toxin expressing cassette; (*), tetracysteine tag; E1–4, exons 1–4. Coding exons are colored in blue, and 5′UTR exons are open rectangles.

(C) Survival analysis of offspring from heterozygous matings of the KI line (top panel) and the KO line (bottom panel). The gray shaded area represents a Mendelian distribution.

(D) Force-plate actometer analysis of male littermate KO and wild-type mice from a continuous single trial recording of 30 min. Data were analyzed in three 10 min frames, and two-way ANOVA and Bonferroni post hoc tests were used for statistical and pairwise analysis (see Table S1 for detailed values), *$p < 0.05$, **$p < 0.01$, ***$p < 0.001$.

versa), and *C. elegans* contains a single *ELKS* gene. The *Drosophila* genome encodes a single related gene called *bruchpilot* in which the C-terminal ELKS sequence that interacts with the PDZ domain of RIMs is replaced by a larger, unrelated sequence (Monier et al., 2002; Wagh et al., 2006). ELKS proteins are ubiquitously expressed in all tissues, similarly to α-liprins (Monier et al., 2002; Nakata et al., 2002; Serra-Pages et al., 1998; Wang et al., 2002), but are most abundant in neurons, where they are enriched in active zones (Ohtsuka et al., 2002; Wang et al., 2002).

Three types of functional studies were carried out on ELKS proteins: genetic experiments in *C. elegans* and *Drosophila*, overexpression and microinjection experiments in cultured neurons, and transfection and siRNA experiments in *Drosophila* and non-neuronal cells. In *C. elegans*, deletion of ELKS causes no detectable phenotype (Deken et al., 2005), although a nonlethal effect of

the deletion on synaptic transmission may be present. The latter suggestion is supported by the finding that a gain-of-function mutation in *syd-2* (the *C. elegans* α-liprin homolog) requires ELKS for its effect on synapse formation (Dai et al., 2006). In *Drosophila*, RNAi-induced knockdown of *bruchpilot* resulted in a walking deficit and unstable flight (Wagh et al., 2006), and genetic deletion of *bruchpilot* led to a complete loss of the dense T-bar projections at the active zone of larval neuromuscular junctions (Kittel et al., 2006). Moreover, overexpressed GFP-tagged presynaptic Ca^{2+} channels were mislocalized, and neurotransmitter release was decreased in neuromuscular junctions of the *bruchpilot* mutant larvae. In cultured rat neurons, microinjection experiments suggested that ELKS2α/CAST is essential for neurotransmitter release, and that the interaction of ELKS2α with RIMs and piccolo/bassoon is required for active zone function and release (Takao-Rikitsu et al., 2004). Furthermore, transfections and siRNA experiments in nonneuronal cells indicated that ELKS is involved in the Rab6-dependent vesicle traffic in the trans-Golgi apparatus (Monier et al., 2002), in insulin secretion (Ohara-Imaizumi et al., 2005), and in the regulation of IκB kinase in lymphocytes (Ducut Sigala et al., 2004). Thus, various approaches led to diverse views of ELKS function.

In the present experiments, we have used mouse genetics, electrophysiology, electron microscopy, and behavioral analysis to systematically examine the function of ELKS2α in mice. Specifically, we analyzed conditional and constitutive ELKS2α knockout (KO) mice. We show that deletion of ELKS2α/CAST did not impair release, but instead caused a major increase in inhibitory synaptic responses and in the size of the readily-releasable pool (RRP) of vesicles at inhibitory synapses. Importantly, deletion of ELKS2α induced no changes in the overall structure of these synapses, nor did it affect excitatory synapses. Thus, our data suggest that ELKS2α/CAST has a regulatory function in synaptic vesicle priming at the active zone of inhibitory synapses.

RESULTS

Generation of Conditional ELKS2α KO Mice

We generated conditional ELKS2α KO mice using homologous recombination in embryonic stem (ES) cells, targeting the first coding exon of the *ELKS2* gene (exon 3, Figure 1B). For this purpose, we isolated a genomic clone containing exon 3 of the *ELKS2* gene, and constructed a targeting vector in which we flanked exon 3 with loxP sites, inserted a neomycin resistance cassette surrounded by frt sites in a nonconserved sequence in intron 3, and employed a diphtheria toxin-expressing cassette for negative selection. We then used homologous recombination in R1 ES cells to introduce the mutant allele into the mouse genome, and generated chimeric mice carrying the mutant *ELKS2* locus by blastocyst injection. After germline transmission of the mutant *ELKS2* allele, we removed the neomycin resistance gene by flp recombination to produce the conditional KO mouse line, and created a constitutive mouse KO by cre recombination in the male germline. Correct gene targeting was confirmed by Southern blotting and PCR in ES cell clones and mutant mice (Figures S1A–S1C available online).

Both conditional (referred to as ELKS2α$^{f/f}$ in the figures) and constitutive ELKS2α KO mice (referred to as ELKS2α$^{-/-}$) were viable and fertile. Survival ratios of offsprings of heterozygous matings revealed a normal Mendelian distribution of genotypes in the offspring at postnatal day 21 for both conditional and constitutive KO mice (Figure 1C; $p > 0.5$ for both lines measured by χ test for the offspring distribution). All analyses of mutant mice described below were performed on littermate offspring from heterozygous matings (for the constitutive KO), or on neurons cultured from homozygous conditional KO mice that were infected with lentivirus expressing either cre recombinase (test) or recombination-deficient, truncated cre (control). Wherever possible, the experimenter was unaware of the genotype of the samples analyzed.

As an initial screen for abnormalities of neural function, we measured the behavior of ELKS2α KO mice with a force-plate actometer. When a mouse is placed in this instrument, the actometer tracks the movement of the center of force in two axes as the mouse explores the novel environment of the plate (Fowler et al., 2001). This test allows a quantitative assessment of locomotion, exploratory behavior, motor coordination, and stereotypy. We examined three pairs of adult littermate male ELKS2α KO and wild-type mice, using a single trial of 30 min, and analyzed their movements in three 10 min frames (Figure 1D and Table S1 available online). Interestingly, ELKS2α KO mice exhibited normal locomotor activity during the first 10 min of the trial (as expressed by the distance traveled on the plate), but displayed a significant increase in activity afterwards. Furthermore, the spatial confinement of the ELKS2α KO mice was largely decreased in the last 10 min, and the ELKS2α KO mice showed a strong reduction in the number of low mobility bouts in the same time period (Figure 1D), without signs of ataxia or stereotypy (Figure S2). Together, these data suggest that deletion of ELKS2α produces a significant increase in exploratory drive.

The *ELKS2* Gene Encodes Multiple ELKS2 Isoforms

We confirmed by immunoblotting of whole-brain homogenates from wild-type (ELKS2α$^{+/+}$) and ELKS2α KO mice that ELKS2α was absent in homozygous ELKS2α KO mice (Figures 2A, S3A, and S3B). We then measured the relative levels of more than 20 synaptic proteins by quantitative immunoblotting using ^{125}I-labeled secondary antibodies, but observed no significant change in any protein other than ELKS, in particular not in other active zone proteins (Figure 2B, also see Figures S6A and S6B). A polyclonal antiserum that reacts with both ELKS1 and ELKS2 proteins (for ELKS antibody specificities, see Figure S1D) revealed that the 130 kD ELKS band was reduced to 52% ± 3% (n = 3) in the ELKS2α KO mice (Figure 2B), demonstrating that ELKS2α accounts for approximately half of the total ELKS protein in brain.

We next examined the expression patterns of ELKS proteins in multiple brain areas as a function of development in wild-type and ELKS2α KO mice (Figures S3A and S3B). ELKS2α is expressed throughout the forebrain, but is undetectable in the cerebellum, the brain stem, and the spinal cord (Figure S3A). This expression pattern is compatible with the mRNA distribution of ELKS2 isoforms in the Allen Brain Atlas (www.brain-map.org), and that published with in situ data (Ko et al., 2006), which demonstrate that ELKS2 is expressed in pyramidal and interneurons throughout the forebrain, including area CA1 of the hippocampus.

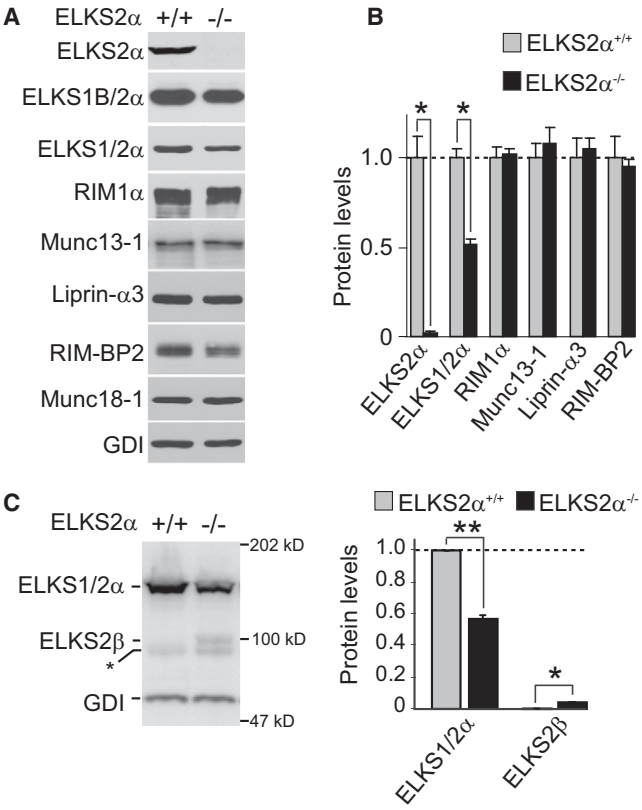

Figure 2. Protein Composition of Brains of ELKS2α KO and Littermate Wild-Type Control Mice

(A) Western blotting using chemiluminescence for detection of ELKS1, ELKS2, and multiple active zone proteins in ELKS2α KO and wild-type littermate brain homogenates.

(B) Quantitation of brain proteins of ELKS2α KO and wild-type littermate control mice at P50–P55 using ^{125}I-labeled secondary antibodies (n = 3; also see Figures S6A and S6B).

(C) Sample western blot (left) with ^{125}I-labeled secondary antibodies and quantitation (right) of the relative expression levels of ELKS isoforms in 50-day-old ELKS2α KO mice and wild-type littermate controls (n = 3; also see Figure S3D). Protein levels are expressed as the percentage of total ELKS1+ ELKS2α in wild-type mice.

All data are shown as mean ± SEM, *p < 0.05, **p < 0.01.

Unexpectedly, in examining immunoblots from ELKS2α KO mice, we detected a new ELKS2 isoform of 95 kD (referred to as ELKS2β; Figures S3A and S3B). In wild-type mice, ELKS2β is expressed at low levels during early postnatal development (~4% of total ELKS protein), and becomes undetectable after postnatal day 20 (Figure S3B). In ELKS2α KO mice, however, ELKS2β remains expressed at constant, low levels throughout adulthood (~4% of total ELKS protein), as evidenced by immunoblotting with two different ELKS antibodies and quantitation with ^{125}I-labeled secondary antibodies (Figures 2C and S3D). ELKS2β, like other ELKS isoforms, is biochemically insoluble (Figure S3C).

Analysis of genomic and cDNA sequences revealed that ELKS2β is produced by an internal promoter in the *ELKS2* gene that drives expression of an ELKS2β-specific 5′ exon (called exon 1″) located 400 base pairs upstream of exon 6 (Figure S4A and Wang et al., 2002). ELKS2β is conserved in rat and human *ELKS2* genes (amino acid sequence identity of the ELKS2β-specific exon: mouse versus rat = 96%, mouse versus human = 67%), and can be identified by immunoblotting in mouse and rat brain (Figure S3E). Moreover, database analyses revealed that the *ELKS2* gene additionally contains alternatively spliced 3′ exons that encode a novel C-terminal splice variant that lacks the RIM-binding sequence (for detailed sequences and database information, see Figure S5). Thus, analogous to the 3′ exons in the *ELKS1* gene that produce ELKS1A and ELKS1B variants (Wang et al., 2002), the *ELKS2* gene produces C-terminal ELKS2A and ELKS2B isoforms. Together with the N-terminal α- and β-variants, the ELKS2 gene therefore expresses four principal isoforms (ELKS2αA, 2αB, 2βA, and 2βB), of which ELKS2αB vastly predominates (Figure S4B). Preliminary analyses of the ELKS1 gene indicate that it also produces additional α- and β-forms, resulting in a similar set of four isoforms (ELKS1αA, 1αB, 1βA, and 1βB; P.S.K. and T.C.S, unpublished data).

Increased Evoked Inhibitory Synaptic Responses in ELKS2α KO Mice

To determine whether deletion of ELKS2α alters neurotransmitter release, we monitored the effect of the constitutive ELKS2α KO on synaptic transmission in acute brain slices in a systematic set of experiments (for numerical results of all electrophysiological slice experiments, see Table S2).

First, we characterized excitatory synaptic transmission at Schaffer collateral synapses in the hippocampal CA1 region, but detected no significant difference between ELKS2α KO and littermate control mice in the frequency and amplitude of spontaneous miniature excitatory postsynaptic currents (mEPSCs, Figure 3A), in input/output curves (Figure 3B), in paired-pulse ratios (Figure 3C), or in synaptic depression in response to a stimulus train (25 stimuli at 14 Hz, Figure 3D).

Second, we characterized inhibitory synaptic transmission in synapses formed by interneurons onto pyramidal neurons in area CA1 of the hippocampus. We detected no change in spontaneous miniature inhibitory postsynaptic currents (mIPSCs; Figure 4A), but observed a large increase in the amplitudes of evoked IPSCs in ELKS2α KO mice (Figure 4B). Input/output curves revealed an almost 2-fold enhancement in IPSC amplitudes at all stimulus intensities (Figure 4B and Table S2).

Third, we measured short-term synaptic plasticity in inhibitory synapses. The strong increase in inhibitory neurotransmitter release in ELKS2α-deficient synapses could result from an increase in the number of Ca^{2+}-responsive vesicles (i.e., an increase in the RRP), or an increase in release probability (P_r), which in turn could be due to an increase in Ca^{2+} influx during an action potential, and/or an increase in Ca^{2+} sensitivity of release-ready vesicles. To test P_r, albeit indirectly, we examined in ELKS2α-deficient synapses two forms of short-term synaptic plasticity: paired-pulse depression (Figure 4C), and use-dependent depression during a 10 Hz stimulus train (Figure 4D). Short-term synaptic plasticity is determined, at least in part, by changes in P_r, such that an increase in P_r leads to a decrease in facilitation (or increased depression), and vice versa. In both forms of short-term plasticity tested, we observed a modest increase in depression, indicating a small change in P_r (Figures 4C and 4D). This change, although significant, is proportionally

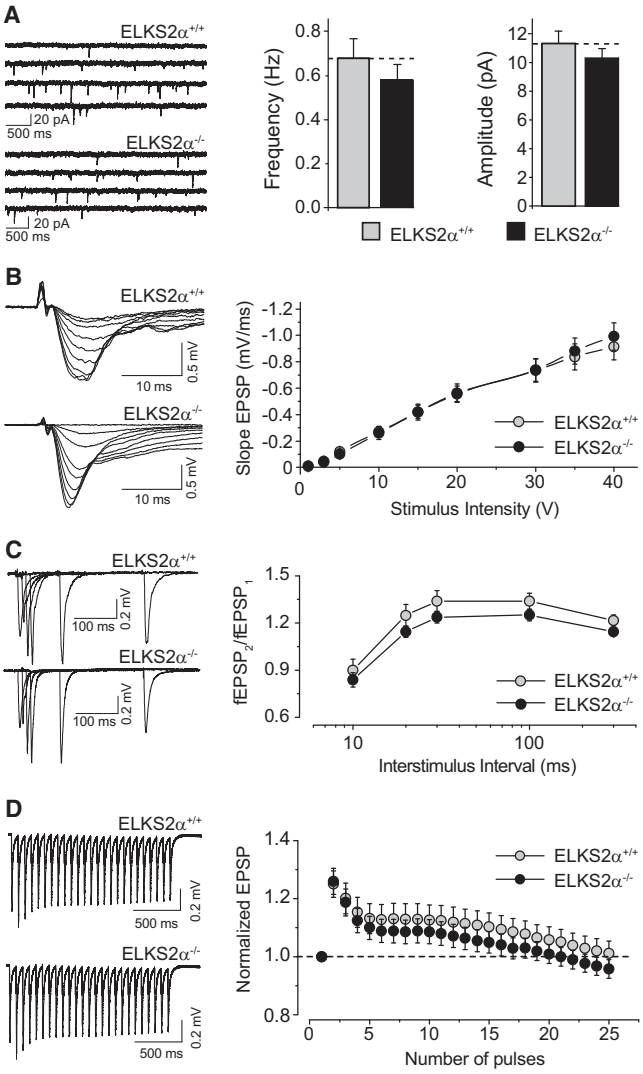

Figure 3. Excitatory Synaptic Transmission at Schaffer Collateral-CA1 Pyramidal Cell Synapses in Wild-Type and ELKS2α KO Mice

(A) Sample traces (left) and quantitative analysis (right) of mEPSC activity in wild-type and ELKS2α KO mice.

(B) Input/output function of ELKS2α KO and wild-type mice, showing the EPSP slope as a function of stimulus intensity.

(C) Paired-pulse responses superimposed after subtraction of the first pulse at 10, 20, 30, 100, and 300 ms interstimulus intervals (ISI).

(D) Synaptic responses evoked by a burst of 25 stimuli at 14 Hz.

All quantitative analyses are reported as means ± SEM, and no statistically significant difference was observed in (A)–(D).

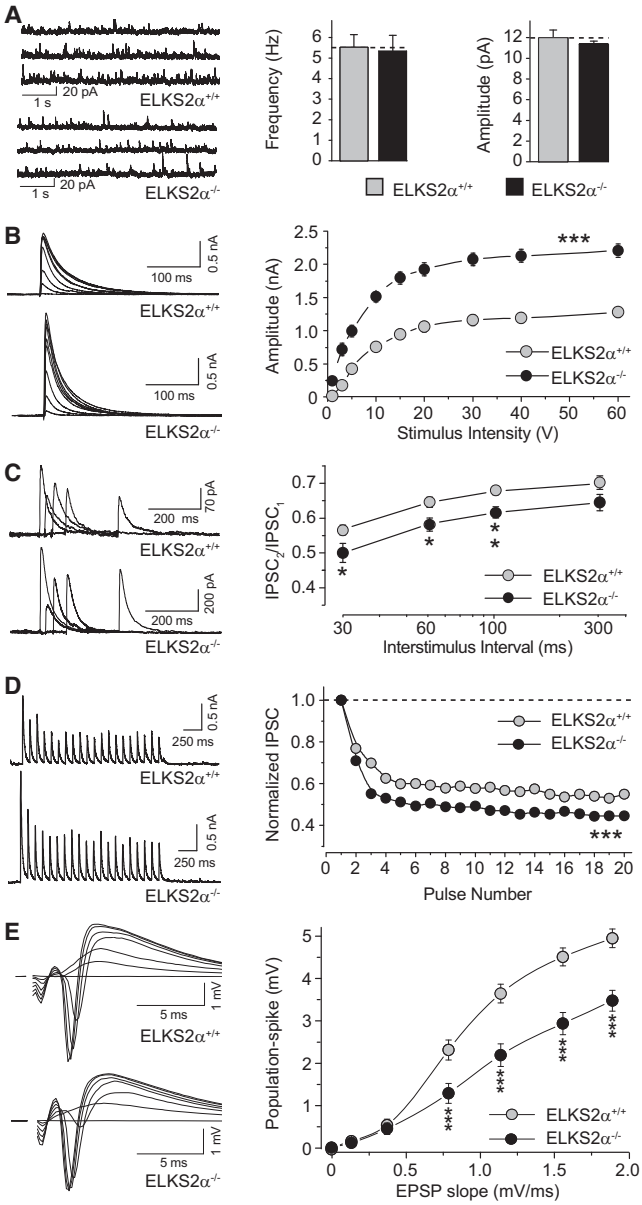

Figure 4. Inhibitory Synaptic Transmission at CA1 Pyramidal Cells in Wild-Type and ELKS2α KO Mice

(A) Sample traces (left) and summary data (right) of mIPSC activity in wild-type and ELKS2α KO mice.

(B) Evoked IPSC amplitudes as a function of stimulus intensity plotted as input/output curves in inhibitory synapses. (***), sample values of statistical significance: stimulus intensity 1V, $p < 0.002$; 20V, $p < 0.001$; 60V, $p < 0.001$.

(C) Paired-pulse responses superimposed after subtraction of the first pulse at 20, 50, 100, and 300 ms ISIs. Statistical significance: *$p < 0.05$, **$p < 0.01$.

(D) Synaptic responses and normalized summary data evoked by a burst of 20 stimuli at 10 Hz. (***), statistical significance of IPSC train ratio, $20^{th}/1^{st}$ peak: $p < 0.001$.

(E) Excitatory postsynaptic potential-spike coupling (E-S coupling) in wild-type and ELKS2α KO mice, where the input is the excitatory synaptic response and the output is the population-spike. All graphs show means ± SEMs, ***$p < 0.001$.

smaller than the increase in IPSC amplitudes (Figure 4B), suggesting that the majority of the increase in the IPSC amplitudes cannot be accounted for by a change in P_r, but could be due to an increase in the RRP, as confirmed below in cultured neurons.

Fourth, we investigated whether ELKS2α participates in long-term synaptic plasticity at inhibitory synapses. A subclass of inhibitory interneurons in area CA1 of the hippocampus exhibits a presynaptic form of inhibitory long-term depression that depends

on endocannabinoids (i-LTD) and on the presynaptic active zone protein RIM1α (Chevaleyre and Castillo, 2003; Chevaleyre et al., 2007). However, we elicited a similar magnitude of i-LTD in ELKS2α KO and wild-type littermate mice (Figure S7), suggesting that ELKS2α does not participate in this form of long-term plasticity.

Finally, we tested whether the enhanced inhibitory inputs onto CA1 pyramidal cells in the ELKS2α KO mice alters the excitatory/inhibitory balance of these neurons. In acute brain slices, excitatory postsynaptic potential-spike coupling (E-S coupling) is a direct way to test how excitatory and inhibitory inputs modulate pyramidal cell excitability. Extracellular field stimulation was used to coactivate both inhibitory and excitatory inputs onto CA1 pyramidal cells, and post-spike potentials (output) were plotted as a function of excitatory synaptic responses (input). Compellingly, we found that in ELKS2α KO mice, E-S coupling was significantly decreased, reflected by the reduced population-spike potential at a given excitatory input (Figure 4E).

Effect of the ELKS2α Deletion on Synapse Structure

The striking increase in inhibitory synaptic strength in ELKS2α KO mice raises the possibility that the number of vesicles docked at the active zone may be increased in these mutant mice. To test this possibility, we examined the ultrastructure of wild-type and ELKS2α-deficient synapses by electron microscopy (Figure 5). Excitatory and inhibitory synapses were analyzed separately after classification into "symmetric" and "asymmetric" synapses, a method that has been shown to reliably distinguish excitatory (asymmetric, Figure 5A) and inhibitory (symmetric, Figure 5B) synapses onto hippocampal pyramidal cells (Megias et al., 2001).

ELKS2α-deficient synapses exhibited no significant change in the number of vesicles that are either docked at the active zone or close to the active zone, suggesting that the augmented inhibitory synaptic transmission is not due to an increase in docked vesicles in the ELKS2α KO mice (Figure 5; Table S3). The only change we observed was a small but significant reduction in vesicle numbers per bouton in both symmetric and asymmetric synapses (Figure 5). Previous studies on synapsin KO mice showed that even a 50% reduction in the number of synaptic vesicles produces a relatively modest decrease in neurotransmitter release (Rosahl et al., 1995), suggesting that the decrease in synaptic vesicle numbers observed in the ELKS2α-deficient synapses by itself is unlikely to have a functionally detectable effect.

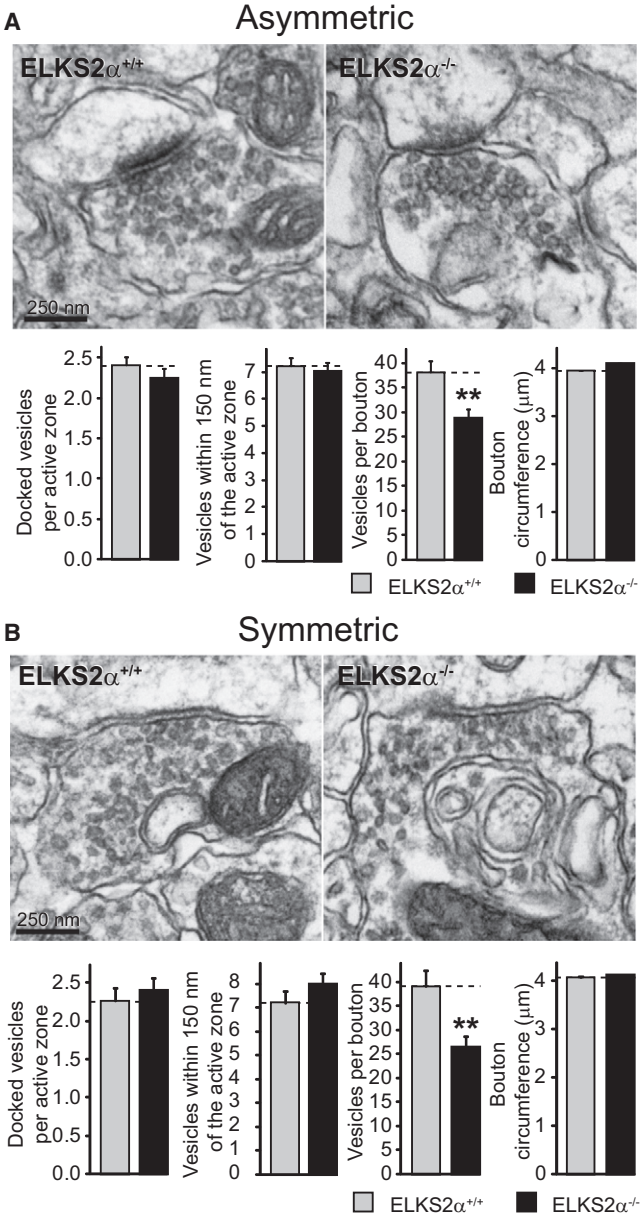

Figure 5. Ultrastructural Analysis of Synaptic Morphology in Area CA1 of the Hippocampus in ELKS2α KO and Littermate Control Mice

(A) Representative images (top) and quantitative analysis (bottom) of asymmetric, excitatory synapses.

(B) Analysis of symmetric, inhibitory synapses.

All data are shown as means ± SEMs, **$p < 0.01$.

Supportive Evidence for an Interaction between ELKS2α and RIM1α

Active zones are insoluble structures that are tightly attached to the presynaptic plasma membrane, where ELKS binds to three other active zone components: α-liprins (Ko et al., 2003); RIMs (Wang et al., 2002); and piccolo/bassoon (Takao-Rikitsu et al., 2004). To test whether global changes in the composition of active zones contribute to the physiological phenotype we observed, we measured whether the solubility of ELKS-interacting proteins and other synaptic proteins is changed in ELKS2α KO mice. We prepared synaptosomes, and separated them into pellet (P2) and supernatant (S2) fractions (Wang et al., 2002). Protein quantitations revealed that the ELKS2α KO induced a selective increase of RIM1α in the soluble S2 fraction (Figures 6A and 6B, wild-type 100.0% ± 2.2%, KO 127.2% ± 2.9%, n = 3, $p < 0.05$; a second antibody reveals a similar trend [Table S4]; note that only ~12% of RIM1α is soluble in wild-type mice). The levels of all other proteins in the S2 and P2 fractions were identical between KO and wild-type littermate control mice, except for a small decrease of synaptotagmin-1 in the P2 fraction (Figures 6 and S6C and Table S4). This observation supports

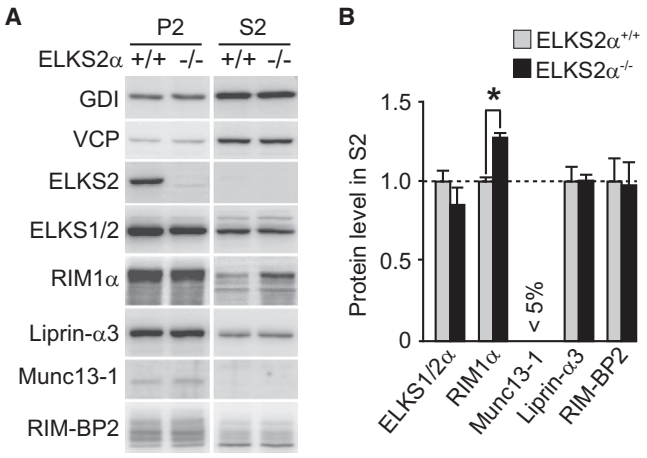

Figure 6. Increased Solubility of RIM1α in ELKS2α KO Brain Homogenates

(A) Sample western blots with ^{125}I-labeled secondary antibodies of the crude synaptosomal pellet fraction (P2) and the synaptosomal supernatant (S2).

(B) Quantitation of protein levels in S2 of three ELKS2α KO mice and wild-type littermate controls. For a complete analysis see Figure S6C and Table S4. All data are shown as mean ± SEM, *p < 0.05.

previous reports that suggested biochemical interactions between RIM and ELKS (Lu et al., 2005; Wang et al., 2002). It is also consistent with the finding that ELKS in *C. elegans* is displaced from active zones by overexpression of the RIM PDZ domain (Deken et al., 2005), and that RIM1α in cultured neurons is mislocalized when it is cotransfected with the ELKS2 C terminus (Ohtsuka et al., 2002). Taken together, our observations and previous studies suggest that ELKS2α physiologically interacts with RIM1α, but that no global reorganization of active zones occurs upon constitutive deletion of ELKS2α.

Conditional Deletion of ELKS2α in Cultured Neurons Also Increases Inhibitory Synaptic Transmission

To probe the function of ELKS2α by an independent physiological approach, we cultured hippocampal neurons from newborn homozygous conditional ELKS2α KO mice, and infected the neurons at 3–4 days in vitro (DIV) with a lentivirus expressing GFP-tagged cre recombinase (ELKS2α$^{f/f}$:cre), or a control virus expressing an inactive mutant of GFP-cre recombinase (ELKS2α$^{f/f}$:control, see Ho et al., 2006). This approach ablates ELKS2α expression postnatally in differentiated neurons, and thereby controls for compensatory effects induced during embryonic development by the constitutive KO of a gene. The percentage of infected neurons was monitored by GFP fluorescence, and the experiments described below were performed in cultures where no noninfected neurons could be detected. The test and control neurons analyzed are identical except for the presence or absence of ELKS2α, as confirmed by immunoblotting (Figure S8A). Moreover, morphological analyses of ELKS2α-deficient and control neurons at DIV13–16 showed that the excitatory and inhibitory synapse density and the synaptic fine structure are unchanged after conditional deletion of ELKS2α (Figures S9 and S10, Table S5).

Extensive electrophysiological measurements of synaptic responses in ELKS2α-deficient and control neurons revealed a phenotype very similar to that observed in brain slices. Specifically, we found that the postnatal deletion of ELKS2α had no significant effect on the frequency or size of spontaneous mIPSCs (Figure 7A), but caused an ~30% increase in the amplitude, and a ~40% increase in the synaptic charge transfer, of evoked IPSCs (Figure 7B; for numerical values, see Table S6). Importantly, this increase in inhibitory synaptic transmission could be rescued to control levels with full-length ELKS2α (Figures 7B and S8C, and Supplemental Experimental Procedures). To analyze the kinetics of synaptic responses, we fitted the integrated charge transfer during synaptic responses to a two-component exponential function with two time constants, τ_{fast} and τ_{slow}, that divide the release into a fast and a slow constituent, A_{fast} and A_{slow} (Pang et al., 2006). These kinetic parameters are descriptive tools characterizing the time course of release, and are not directly related to the fast and the slow components of release (Geppert et al., 1994). We found that the time constants and the relative contributions of their underlying constituents were unchanged in ELKS2α-deficient synapses, indicating that the deletion of ELKS2α does not alter the kinetics of release (Figure S11).

Because we observed a modest increase of P_r at inhibitory synapses in hippocampal slices, we also characterized short-term plasticity and Ca^{2+} responsiveness after postnatal deletion of ELKS2α. Responses to paired-pulse stimulation (Figure 7C) and brief stimulus trains (20 action potentials at 10 Hz, Figure S11C) uncovered only a nonsignificant trend to increased depression in ELKS2α-deficient synapses. These experiments support the notion that the small increase in P_r observed in acute brain slices was not fully responsible for the increase in inhibitory synaptic transmission in ELKS2α KO mice. Moreover, we observed no change in the amount of delayed release after a short 10 Hz stimulus train (Figure S11D), which represents a form of asynchronous release (Maximov et al., 2007; Maximov and Südhof, 2005). Ca^{2+} responsiveness measured by titration of the extracellular Ca^{2+} concentration of these synapses revealed an exponential relationship between Ca^{2+} and release in the ELKS2α-deficient and control neurons (Figure 7D, fitted Ca^{2+} cooperativity: 2.04 ± 0.22 for control; n = 5 cells, 1.93 ± 0.28 for KO, n = 6 cells), without a change in the apparent Ca^{2+} dependence of release (Table S6). Taken together, these observations suggest that Ca^{2+}-triggering of release, either by an increase in Ca^{2+} influx or the vesicular Ca^{2+} sensitivity, is normal in the absence of ELKS2α.

Since the expression of ELKS2β is slightly increased in ELKS2α KO mice and in cultured ELKS2α-deficient neurons (Figures 2 and S8A), it is conceivable that the small ELKS2β increase in these conditions mediates the increase in inhibitory synaptic transmission observed in the ELKS2α KO mice. To test this possibility, we overexpressed ELKS2β in wild-type neuronal cultures (Figure S8B), but detected no increase in evoked inhibitory responses at synapses (Figures S12A and S12B, Table S6).

Finally, we hypothesized that the increased inhibitory synaptic strength in ELKS2α KO neurons might alter the excitability of the neuronal network formed by these neurons, similar to the E-S coupling depression observed in area CA1 of ELKS2α KO mice

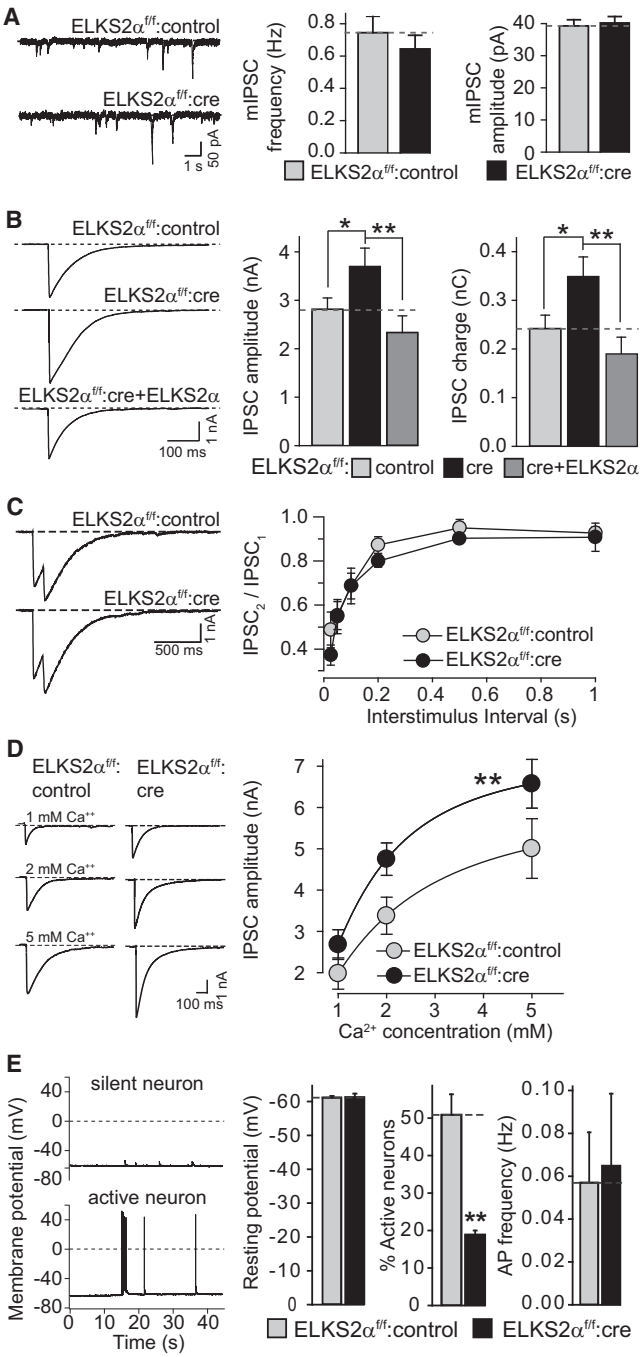

Figure 7. Inhibitory Synaptic Transmission in Conditional ELKS2α KO Synapses in Mixed Hippocampal Cultures

(A) mIPSC recordings in cultured ELKS2α KI neurons after lentiviral cre recombinase infection (conditional KO, ELKS2α$^{f/f}$:cre) or infection with a inactive control lentivirus (control, ELKS2α$^{f/f}$:control).

(B) Evoked IPSC recordings of conditional KO neurons infected with control lentivirus, cre-recombinase expressing lentivirus, or lentivirus coexpressing both cre-recombinase and full-length ELKS2α rescue protein. One-way ANOVA with Newman-Keuls multiple comparison was used for pairwise comparisons; *p < 0.05, **p < 0.01.

(C) Paired-pulse recordings in KO and control neurons at various ISIs.

(D) Evoked inhibitory synaptic transmission measured as a function of the extracellular Ca^{2+} concentration measured at 1, 2, and 5 mM extracellular Ca^{2+}. **p < 0.01 for genotype variation (two-way ANOVA).

(E) Network activity in cultured control and ELKS2α KO neurons. Neurons were categorized in "silent" and "active" groups based on the absence or presence of spontaneous action potentials (APs), respectively.

All data are shown as means ± SEMs, **p < 0.01.

(Figure 4E). The occurrence of spontaneous action potentials in a fraction of cultured hippocampal neurons can be used to divide them in active and silent neurons, and reflects the excitability of these cultured neuronal networks. When we compared the number of active neurons in control and ELKS2α-deficient synapses, we found a significant reduction in the number of active neurons in the absence of ELKS2α, but the resting membrane potential and the frequency of spontaneous action potentials in active neurons were unchanged (Figure 7E). These observations suggest that the increased inhibition in the absence of ELKS2α leads to increased silencing of the neuronal network.

Deletion of ELKS2α Increases the RRP of Inhibitory Synapses

The increase in neurotransmitter release in ELKS2α-deficient inhibitory synapses could result from an increase in the number of Ca^{2+}-responsive vesicles at the active zone (i.e., an increase in the RRP), or an increase in the P_r. Since we already largely excluded a change in P_r as a major factor in the phenotype (see above), we examined the RRP, which can be directly tested in cultured neurons using application of hypertonic sucrose. Hypertonic sucrose is thought to stimulate release of the entire RRP at a synapse in a two-phasic reaction: an initial phase of ~15 s during which the RRP is emptied, and a subsequent steady-state phase during which release reflects the continuous recruitment and exocytosis of vesicles in the presence of the hypertonic sucrose (Rosenmund and Stevens, 1996).

To measure the RRP at inhibitory synapses, we applied to cultured ELKS2α-deficient or control neurons 0.2 M, 0.35 M, or 0.5 M sucrose for 30 s, and integrated the synaptic charge transfer of the resulting response. Deletion of ELKS2α increased the inhibitory RRP size monitored with 0.5 M and 0.35 M sucrose, measured as the integrated synaptic charge transfer during the initial 10 s of hypertonic sucrose application (Figure 8A). However, deletion of ELKS2α only had a small effect on release triggered by 0.2 M sucrose and on the steady-state phase of the sucrose response (Figure 8A, right panel), indicating that vesicle recruitment is likely unchanged. As a control for the measurements of the inhibitory RRP, we measured the excitatory RRP. Consistent with the specificity of the ELKS2α KO phenotype for inhibitory synapses in acute slices (Figures 3 and 4), we detected no change in the RRP of excitatory synapses, or in mEPSCs (Figure S13). Moreover, as shown above for action-potential-evoked responses, the effect of the ELKS2α deletion on inhibitory RRP size was not due to the small increase in ELKS2β in the mutant synapses because ELKS2β overexpression had no effect on inhibitory RRP size (Figure S12C).

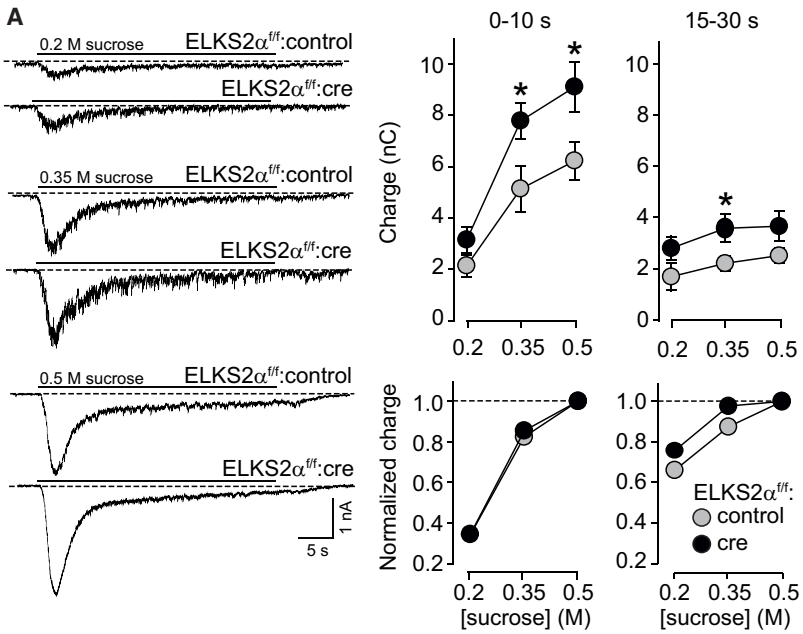

Figure 8. Conditional ELKS2α KO Increases the RRP in Inhibitory Synapses

(A) Quantitative analysis of the RRP size in inhibitory synapses of conditional ELKS2α KO neurons infected with either control or cre-recombinase expressing lentivirus. The RRP size was measured by application of three concentrations of hypertonic sucrose; synaptic charge transfer was then quantified during the first 10 s (left) and during the steady-state phase (15–30 s, right). Absolute (top) and normalized (bottom) values are shown. All data are reported as mean ± SEM, *$p < 0.05$.

(B) Active zones consist of a dense protein network (represented in blue; see Figure 1A for protein constituents) with depressions that form "priming slots" for synaptic vesicles. Our data advocate a hypothetical model wherein these slots can be closed/gated, and upon slot opening the vesicles become available for priming and fusion. ELKS2α and syntaxin-1 in its open confirmation (Gerber et al., 2008) are negative and positive regulators, respectively, of slot opening, keeping the vesicles from joining the pool of vesicles available to the RRP. The exact molecular mechanism by which ELKS2α decreases inhibitory synaptic transmission remains to be elucidated.

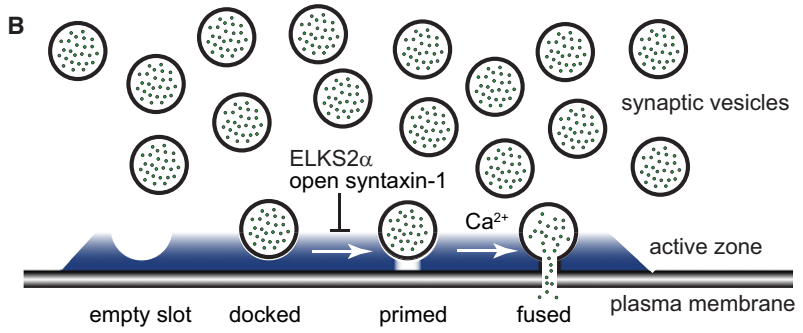

DISCUSSION

The active zone is a central component of the neurotransmitter release machinery that not only represents the place where vesicles dock and fuse, but also mediates presynaptic plasticity. For example, the two interacting active zone proteins RIM and Munc13 are essential for synaptic vesicle priming and fusion, and additionally account for the majority of presynaptic plasticity, although with differential roles (Calakos et al., 2004; Castillo et al., 2002; Chevaleyre et al., 2007; Kaeser et al., 2008; Rhee et al., 2002; Rosenmund et al., 2002; Schoch et al., 2002). Despite the importance of the active zone, the roles of many active zone proteins in vesicle docking and priming and in regulating short- and long-term presynaptic plasticity remain unknown. Moreover, the mechanisms involved are only now beginning to be elucidated. In the present study, we examined the function of ELKS2α, an active zone protein that constitutes a central component of the active zone protein network (Ohtsuka et al., 2002; Wang et al., 2002). We analyzed the effects of constitutive and conditional deletions of ELKS2α on synaptic vesicle docking and priming and on synaptic plasticity. Our major finding is that, surprisingly, ELKS2α restricts inhibitory synaptic transmission. Its deletion produces a large increase in inhibitory synaptic strength without causing detectable impairments in other synaptic parameters, except for a small decrease in synaptic vesicle numbers. In view of previous studies, our findings are unexpected, as they suggest that ELKS2α is not an essential building block of the release machinery, but rather a regulatory component that gates access to this machinery.

Our results raise three questions. (1) Are our results valid, given that they appear to contradict much of what has been published previously about ELKS2α? (2) If our results are valid, how does deletion of ELKS2α increase inhibitory synaptic transmission? (3) What are the implications of our data for the structure and function of the active zone?

(1) The identification of ELKS as a central component of the active zone led to the expectation that it would act as glue that holds the active zone together (Ko et al., 2003; Ohtsuka et al., 2002; Takao-Rikitsu et al., 2004; Wang et al., 2002). Indeed, microinjection and overexpression experiments in neurons appeared to support this hypothesis (Takao-Rikitsu et al., 2004). However, interpretation of these experiments is difficult because introduction of high levels of recombinant proteins into neurons likely has multiple effects on these neurons, in addition to specifically altering ELKS function. In our physiological and morphological analyses, we employ two independent approaches to characterize the ELKS2α KO phenotype: we analyze synaptic transmission in adult mice after constitutive deletion of *ELKS2* (Figures 1–6 and Figures S1–S7), and in cultured neurons from newborn mice after conditional deletion of ELKS2α (Figures 7, 8, and S8–S13). Both analyses uncovered similar phenotypes with a prominent and selective increase in inhibitory synaptic responses, without major alterations in the fine structure of the

synapse, thus making an artifact unlikely. Moreover, the agreement of the results obtained after constitutive KO of ELKS2α in mice and after conditional postnatal deletion of ELKS2α in differentiated neurons argues against developmental compensatory processes during embryonic development, and against genetic background contributions. We did detect a small increase (~4% of total ELKS levels) in the concentration of a novel ELKS2β isoform that we identified in the present study, but this increase did not account for our findings because overexpressed ELKS2β did not induce any functional changes in inhibitory synapses (Figure S12). Moreover, we show that the increase in inhibitory synaptic transmission can be fully rescued by viral expression of ELKS2α.

It should be noted that, to our knowledge, no other mouse mutant has previously been shown to increase the size of the RRP, suggesting that this is a highly specific phenotype. The only protein that has been associated with an inhibitory effect on priming is tomosyn, a synaptic protein that inhibits SNARE complex formation through its interaction with syntaxin-1 (Pobbati et al., 2004). In *C. elegans* synapses, tomosyn inhibits priming to an extent that is similar to the one we observe in the ELKS2α KO mice (Gracheva et al., 2006). Mice lacking tomosyn show an increase in excitatory synaptic input/output function, and decreased paired-pulse ratios, but the size of the RRP has not been addressed (Sakisaka et al., 2008). In addition, the closed conformation of syntaxin-1 inhibits vesicle priming, but opening this conformation only increases the rate of priming, not the capacity of the RRP (Gerber et al., 2008).

Our observations on ELKS2α are in agreement with the genetic findings made in *C. elegans* in which an ELKS-dependent phenotype was only uncovered upon crossing the ELKS mutants with *syd-2*/α-liprin mutants (Dai et al., 2006; Deken et al., 2005). It is possible that the ELKS deletion in *C. elegans* also causes an increase in inhibitory synaptic strength, which would not have been detected, given the difficulty of electrophysiological analysis in *C. elegans*. Deletion of *bruchpilot* in *Drosophila* suggested that this protein promotes active zone assembly and vesicle release, a very different phenotype compared to our or the *C. elegans* results (Kittel et al., 2006; Wagh et al., 2006). However, most ELKS sequences, including the RIM binding motif, are not conserved in *bruchpilot* (Monier et al., 2002; Wagh et al., 2006), making a functional similarity unlikely. Thus, viewed together, many of the various and diverse previous observations on the function of ELKS-related proteins can be reconciled with the current data.

(2) How does deletion of ELKS2α increase inhibitory synaptic transmission? Our data suggest that a selective increase in the size of the inhibitory RRP at these synapses is involved, without a major change in the releasability of the RRP vesicles (i.e., their Ca^{2+} or sucrose sensitivity; Figures 7D and 8A). Importantly, the amount of morphologically docked vesicles is unchanged in inhibitory synapses in brain slices and in cultured neurons (Figures 5 and S10), as shown by conventional transmission electron microscopy. Furthermore, there is a small but significant increase in depression in the absence of ELKS2α in the slice analysis, which suggests a small increase in P_r (Figure 4), but P_r and Ca^{2+} responsiveness are unchanged in inhibitory synapses after conditional deletion of ELKS2α (Figure 7). Taken together, these findings advocate that docking of synaptic vesicles and Ca^{2+}-triggering of synaptic responses do not undergo major changes upon deletion of ELKS2α, and that the increase in release is mediated by a process acting after docking. Our electron microscopy data, however, have to be interpreted with caution, because it has recently been suggested that aldehyde fixation as used in this study might alter the localization of synaptic vesicles, and that high pressure freezing might be superior to aldehyde fixation for measuring docking of synaptic vesicles (Siksou et al., 2007). Biochemically, we find that although the absolute levels of RIM1α are unchanged in the ELKS2α KO brains, the solubility of RIM1α is slightly but significantly increased (Figure 6). These data are compatible with the observation that ELKS solubility is increased in mice lacking RIM1α and RIM1β (Kaeser et al., 2008), and support previous studies suggesting a biochemical and functional interaction between ELKS and RIM (Dai et al., 2006; Lu et al., 2005; Takao-Rikitsu et al., 2004; Wang et al., 2002). However, the relative amount of soluble RIM1α is small, indicating that the major effects of the ELKS2α deletion are mediated by a different mechanism.

A plausible, parsimonious hypothesis is that ELKS2α, via binding to RIMs and α-liprins, forms a barrier that prevents access of vesicles to release slots in the active zone (Figure 8B, also see Cao et al., 2004). Such a model would imply that priming of vesicles into the RRP, occurring after docking at the active zone, is an independently regulated process, and that vesicle docking does not automatically lead to vesicle priming. ELKS2α and possibly interacting proteins could physically occupy such release slots, thereby blocking access of the vesicle to the presynaptic plasma membranes, which is required for fusion. In such a model, physical slot opening through removal of ELKS and/or its interaction partners would allow vesicles to be added to the RRP. Interestingly, a recent study in which syntaxin-1 is expressed as a knockin (KI) mutation in its "open" confirmation supports such a model, as it increases docking of synaptic vesicles but decreases the RRP size (Gerber et al., 2008). At least two other less parsimonious models could also explain the ELKS2α KO phenotype: instead of being itself the negative regulator of priming, ELKS2α could bind to a different negative regulator. A potential candidate for such a mechanism could be tomosyn as outlined above (Gracheva et al., 2006). Alternatively, different ELKS isoforms could recruit different priming factors with distinct priming activities (such as Munc13s, RIMs, and CAPS; see Augustin et al., 1999; Betz et al., 2001; Calakos et al., 2004; Jockusch et al., 2007) to active zones, and deletion of ELKS2α could affect the recruitment of one specific priming factor versus other priming molecules with lower activity.

We cannot currently differentiate between these three models, both because of intrinsic limitations of our study, and because of our insufficient understanding of other priming factors. It remains unclear why deletion of ELKS2α selectively affects inhibitory synapses. A possible explanation could be that ELKS2α is selectively expressed at these synapses, and other ELKS isoforms are expressed at excitatory synapses, although this explanation is inconsistent with the presence of ELKS2α mRNAs in excitatory neurons. Unfortunately, this cannot be tested at present due to the lack of antibodies suitable for isoform-specific immunocytochemistry. More importantly, our studies are limited

because only one out of multiple ELKS isoforms, accounting for half of the total ELKS protein, has been deleted. ELKS likely performs additional functions at the active zone besides those uncovered here, and these functions may not have been impaired by the loss of half of the total ELKS protein in the ELKS2α KO mice. It seems probable that such additional functions exist because deletion of ELKS1 is early embryonically lethal (P.S.K. and T.C.S., unpublished data), consistent with its ubiquitous nonneuronal expression (Wang et al., 2002). However, this circumstance also makes examining these additional functions difficult, as it would require a complete conditional deletion of all ELKS proteins.

(3) How does ELKS2α contribute to overall active zone function? Docking and priming of synaptic vesicles are processes that are currently under intense investigation. At the mammalian active zone, Munc13s and RIMs have been shown to act as priming factors (Augustin et al., 1999; Betz et al., 2001; Calakos et al., 2004; Schoch et al., 2002) in addition to SNAREs and Munc18-1 (Bronk et al., 2007; Deak et al., 2004, 2009; Gerber et al., 2008; Schoch et al., 2001) (also see Table S7 for an overview of priming molecules). However, the molecular events that underlie priming, or the function of priming in modulating release during plasticity, are not understood. A role for ELKS2α in limiting the size of the RRP at the synapse is consistent with the notion that the active zone is involved in plasticity, as limiting release via ELKS-mediated interactions may provide a substrate for the regulation of release. According to our model (Figure 8B), the biological significance of the ELKS2α-dependent restriction of the RRP would be to allow leeway for regulating release. In support of this, we show that removal of ELKS2α alters the excitability of neuronal networks, and that ELKS2α KO mice exhibit enhanced exploratory behavior (Figures 1, 4, and 7).

Altogether, our data form a basis for mechanistic insights into ELKS action at the active zone. Unanswered questions raised by our data are the following: do ELKS1 and ELKS2 function homologously at active zones? Are they expressed at different types of synapses? What is the mechanism for the increased RRP observed in this study? Do ELKS proteins regulate the abundance or activity of other priming factors? Among other potential uses, the conditional KO mice presented here embody a tool to further evaluate the mechanism of ELKS action and the in vivo importance of specific active zone functions.

EXPERIMENTAL PROCEDURES

Generation of ELKS2 Mutant Mice

Mice were generated according to standard procedures (Ho et al., 2006; Kaeser et al., 2008), targeting exon 3 of the *ELKS2* gene by homologous recombination in R1 ES cells. See Supplemental Experimental Procedures for a detailed description and for genotyping protocols.

Protein Quantitations in Brain Homogenates and in S2 and P2 Fractions

Protein quantitations were done with ^{125}I-labeled secondary antibodies as previously described (Ho et al., 2006). Valosin-containing protein (VCP) and GDP dissociation inhibitor (GDI) were used as internal standards. Fractionation in crude synaptosomal fraction (P2) and synaptosomal supernatant (S2) was essentially performed as previously published (Wang et al., 2002), and are described in detail in the Supplemental Experimental Procedures. Protein contents were adjusted by use of a BCA protein assay. Forty-five micrograms of protein was loaded per lane on standard SDS/Page gels for western blotting.

Force-Plate Actometer Recordings

The movement of the center of force was recorded in a single trial for 30 min in the force-plate actometer as previously described (Fowler et al., 2001). Three 5-month-old male littermate pairs were used, and the mice were exposed to the actometer for the first time during the 30 min trial. A detailed description of the method can be found in the Supplemental Experimental Procedures.

Electrophysiology

Electrophysiological recordings in acute brain slices (Figures 3, 4, and S7) were performed in ELKS2α wild-type and KO littermate mice according to methods that were previously described (Kaeser et al., 2008). ELKS2α KO and wild-type littermates were shipped to Albert Einstein College of Medicine (Bronx, NY) unidentified, and data were acquired and analyzed in a blind fashion. Experiments in cultured hippocampal neurons (Figures 7, 8, and S11–S13) were completed according to previously published methods (Ho et al., 2006; Maximov et al., 2007). In brief, mixed hippocampal cultures were infected with GFP-cre expressing or control virus at DIV2–4, and infection efficiency was monitored by nuclear GFP fluorescence. Recordings were performed at DIV13–16. Detailed methodological descriptions of recordings in acute brain slices and cultured neurons can be found in the Supplemental Data.

Morphology

Immunofluorescent labelings and electron microscopy were essentially performed as described (Ho et al., 2006; Wang et al., 2002). See Supplemental Experimental Procedures for a detailed description.

Miscellaneous

SDS/Page gels and immunoblotting were done according to standard methods (Ho et al., 2006). All data are shown as means ± SEMs. Statistical significance was determined by the Student's t test (two-tailed distribution, paired) unless otherwise stated. All animal experiments were performed according to institutional guidelines.

SUPPLEMENTAL DATA

Supplemental data for this article include Supplemental Experimental Procedures, six tables listing detailed numerical values with statistical analyses for key results, one table listing previous genetic studies investigating vesicle priming, and 13 supplementary figures, and can be found at http://www.cell.com/neuron/supplemental/S0896-6273(09)00719-3.

ACKNOWLEDGMENTS

We would like to thank E. Borowicz, J. Mitchell, I. Kornblum, and L. Fan for excellent technical assistance; Dr. Nils Brose for Munc13 antibodies; Dr. Stephen C. Fowler for advice with the force-plate actometer experiments; and Dr. Robert Hammer for blastocyst injections of ES cells. We are grateful to members of the Südhof lab for comments and advice. This work was supported by grants from the NIH (NINDS 33564 to T.C.S. and DA17392 to P.E.C.), a Swiss National Science Foundation Postdoctoral Fellowship (to P.S.K.), the Irma T. Hirschl Career Scientist Award (to P.E.C.), and a NARSAD Young Investigator Award (to P.S.K.).

Accepted: August 24, 2009
Published: October 28, 2009

REFERENCES

Altrock, W.D., tom Dieck, S., Sokolov, M., Meyer, A.C., Sigler, A., Brakebusch, C., Fassler, R., Richter, K., Boeckers, T.M., Potschka, H., et al. (2003). Functional inactivation of a fraction of excitatory synapses in mice deficient for the active zone protein bassoon. Neuron *37*, 787–800.

Aravamudan, B., Fergestad, T., Davis, W.S., Rodesch, C.K., and Broadie, K. (1999). Drosophila UNC-13 is essential for synaptic transmission. Nat. Neurosci. *2*, 965–971.

Augustin, I., Rosenmund, C., Südhof, T.C., and Brose, N. (1999). Munc13-1 is essential for fusion competence of glutamatergic synaptic vesicles. Nature *400*, 457–461.

Betz, A., Thakur, P., Junge, H.J., Ashery, U., Rhee, J.S., Scheuss, V., Rosenmund, C., Rettig, J., and Brose, N. (2001). Functional interaction of the active zone proteins Munc13-1 and RIM1 in synaptic vesicle priming. Neuron *30*, 183–196.

Bronk, P., Deak, F., Wilson, M.C., Liu, X., Südhof, T.C., and Kavalali, E.T. (2007). Differential effects of SNAP-25 deletion on Ca2+ -dependent and Ca2+ -independent neurotransmission. J. Neurophysiol. *98*, 794–806.

Calakos, N., Schoch, S., Südhof, T.C., and Malenka, R.C. (2004). Multiple roles for the active zone protein RIM1alpha in late stages of neurotransmitter release. Neuron *42*, 889–896.

Cao, Y.Q., Piedras-Renteria, E.S., Smith, G.B., Chen, G., Harata, N.C., and Tsien, R.W. (2004). Presynaptic Ca2+ channels compete for channel type-preferring slots in altered neurotransmission arising from Ca2+ channelopathy. Neuron *43*, 387–400.

Castillo, P.E., Schoch, S., Schmitz, F., Südhof, T.C., and Malenka, R.C. (2002). RIM1alpha is required for presynaptic long-term potentiation. Nature *415*, 327–330.

Chevaleyre, V., and Castillo, P.E. (2003). Heterosynaptic LTD of hippocampal GABAergic synapses: a novel role of endocannabinoids in regulating excitability. Neuron *38*, 461–472.

Chevaleyre, V., Heifets, B.D., Kaeser, P.S., Südhof, T.C., and Castillo, P.E. (2007). Endocannabinoid-mediated long-term plasticity requires cAMP/PKA signaling and RIM1alpha. Neuron *54*, 801–812.

Dai, Y., Taru, H., Deken, S.L., Grill, B., Ackley, B., Nonet, M.L., and Jin, Y. (2006). SYD-2 Liprin-alpha organizes presynaptic active zone formation through ELKS. Nat. Neurosci. *9*, 1479–1487.

Deak, F., Schoch, S., Liu, X., Südhof, T.C., and Kavalali, E.T. (2004). Synaptobrevin is essential for fast synaptic-vesicle endocytosis. Nat. Cell Biol. *6*, 1102–1108.

Deak, F., Xu, Y., Chang, W.P., Dulubova, I., Khvotchev, M., Liu, X., Südhof, T.C., and Rizo, J. (2009). Munc18-1 binding to the neuronal SNARE complex controls synaptic vesicle priming. J. Cell Biol. *184*, 751–764.

Deken, S.L., Vincent, R., Hadwiger, G., Liu, Q., Wang, Z.W., and Nonet, M.L. (2005). Redundant localization mechanisms of RIM and ELKS in Caenorhabditis elegans. J. Neurosci. *25*, 5975–5983.

Ducut Sigala, J.L., Bottero, V., Young, D.B., Shevchenko, A., Mercurio, F., and Verma, I.M. (2004). Activation of transcription factor NF-kappaB requires ELKS, an IkappaB kinase regulatory subunit. Science *304*, 1963–1967.

Fowler, S.C., Birkestrand, B.R., Chen, R., Moss, S.J., Vorontsova, E., Wang, G., and Zarcone, T.J. (2001). A force-plate actometer for quantitating rodent behaviors: illustrative data on locomotion, rotation, spatial patterning, stereotypies, and tremor. J. Neurosci. Methods *107*, 107–124.

Geppert, M., Goda, Y., Hammer, R.E., Li, C., Rosahl, T.W., Stevens, C.F., and Südhof, T.C. (1994). Synaptotagmin I: a major Ca2+ sensor for transmitter release at a central synapse. Cell *79*, 717–727.

Gerber, S.H., Rah, J.C., Min, S.W., Liu, X., de Wit, H., Dulubova, I., Meyer, A.C., Rizo, J., Arancillo, M., Hammer, R.E., et al. (2008). Conformational Switch of Syntaxin-1 Controls Synaptic Vesicle Fusion. Science *321*, 1507–1510.

Gracheva, E.O., Burdina, A.O., Holgado, A.M., Berthelot-Grosjean, M., Ackley, B.D., Hadwiger, G., Nonet, M.L., Weimer, R.M., and Richmond, J.E. (2006). Tomosyn inhibits synaptic vesicle priming in Caenorhabditis elegans. PLoS Biol. *4*, e261.

Ho, A., Morishita, W., Atasoy, D., Liu, X., Tabuchi, K., Hammer, R.E., Malenka, R.C., and Südhof, T.C. (2006). Genetic analysis of Mint/X11 proteins: essential presynaptic functions of a neuronal adaptor protein family. J. Neurosci. *26*, 13089–13101.

Jockusch, W.J., Speidel, D., Sigler, A., Sorensen, J.B., Varoqueaux, F., Rhee, J.S., and Brose, N. (2007). CAPS-1 and CAPS-2 are essential synaptic vesicle priming proteins. Cell *131*, 796–808.

Junge, H.J., Rhee, J.S., Jahn, O., Varoqueaux, F., Spiess, J., Waxham, M.N., Rosenmund, C., and Brose, N. (2004). Calmodulin and Munc13 form a Ca2+ sensor/effector complex that controls short-term synaptic plasticity. Cell *118*, 389–401.

Kaeser, P.S., Kwon, H.B., Chiu, C.Q., Deng, L., Castillo, P.E., and Südhof, T.C. (2008). RIM1alpha and RIM1beta are synthesized from distinct promoters of the RIM1 gene to mediate differential but overlapping synaptic functions. J. Neurosci. *28*, 13435–13447.

Kaufmann, N., DeProto, J., Ranjan, R., Wan, H., and Van Vactor, D. (2002). Drosophila liprin-alpha and the receptor phosphatase Dlar control synapse morphogenesis. Neuron *34*, 27–38.

Kittel, R.J., Wichmann, C., Rasse, T.M., Fouquet, W., Schmidt, M., Schmid, A., Wagh, D.A., Pawlu, C., Kellner, R.R., Willig, K.I., et al. (2006). Bruchpilot promotes active zone assembly, Ca2+ channel clustering, and vesicle release. Science *312*, 1051–1054.

Ko, J., Na, M., Kim, S., Lee, J.R., and Kim, E. (2003). Interaction of the ERC family of RIM-binding proteins with the liprin-alpha family of multidomain proteins. J. Biol. Chem. *278*, 42377–42385.

Ko, J., Yoon, C., Piccoli, G., Chung, H.S., Kim, K., Lee, J.R., Lee, H.W., Kim, H., Sala, C., and Kim, E. (2006). Organization of the presynaptic active zone by ERC2/CAST1-dependent clustering of the tandem PDZ protein syntenin-1. J. Neurosci. *26*, 963–970.

Koushika, S.P., Richmond, J.E., Hadwiger, G., Weimer, R.M., Jorgensen, E.M., and Nonet, M.L. (2001). A post-docking role for active zone protein Rim. Nat. Neurosci. *4*, 997–1005.

Lu, J., Li, H., Wang, Y., Südhof, T.C., and Rizo, J. (2005). Solution structure of the RIM1alpha PDZ domain in complex with an ELKS1b C-terminal peptide. J. Mol. Biol. *352*, 455–466.

Maximov, A., and Südhof, T.C. (2005). Autonomous function of synaptotagmin 1 in triggering synchronous release independent of asynchronous release. Neuron *48*, 547–554.

Maximov, A., Pang, Z.P., Tervo, D.G., and Südhof, T.C. (2007). Monitoring synaptic transmission in primary neuronal cultures using local extracellular stimulation. J. Neurosci. Methods *161*, 75–87.

Megias, M., Emri, Z., Freund, T.F., and Gulyas, A.I. (2001). Total number and distribution of inhibitory and excitatory synapses on hippocampal CA1 pyramidal cells. Neuroscience *102*, 527–540.

Monier, S., Jollivet, F., Janoueix-Lerosey, I., Johannes, L., and Goud, B. (2002). Characterization of novel Rab6-interacting proteins involved in endosome-to-TGN transport. Traffic *3*, 289–297.

Nakata, T., Kitamura, Y., Shimizu, K., Tanaka, S., Fujimori, M., Yokoyama, S., Ito, K., and Emi, M. (1999). Fusion of a novel gene, ELKS, to RET due to translocation t(10;12)(q11;p13) in a papillary thyroid carcinoma. Genes Chromosomes Cancer *25*, 97–103.

Nakata, T., Yokota, T., Emi, M., and Minami, S. (2002). Differential expression of multiple isoforms of the ELKS mRNAs involved in a papillary thyroid carcinoma. Genes Chromosomes Cancer *35*, 30–37.

Ohara-Imaizumi, M., Ohtsuka, T., Matsushima, S., Akimoto, Y., Nishiwaki, C., Nakamichi, Y., Kikuta, T., Nagai, S., Kawakami, H., Watanabe, T., and Nagamatsu, S. (2005). ELKS, a protein structurally related to the active zone-associated protein CAST, is expressed in pancreatic beta cells and functions in insulin exocytosis: interaction of ELKS with exocytotic machinery analyzed by total internal reflection fluorescence microscopy. Mol. Biol. Cell *16*, 3289–3300.

Ohtsuka, T., Takao-Rikitsu, E., Inoue, E., Inoue, M., Takeuchi, M., Matsubara, K., Deguchi-Tawarada, M., Satoh, K., Morimoto, K., Nakanishi, H., and Takai, Y. (2002). Cast: a novel protein of the cytomatrix at the active zone of synapses that forms a ternary complex with RIM1 and munc13-1. J. Cell Biol. *158*, 577–590.

Pang, Z.P., Melicoff, E., Padgett, D., Liu, Y., Teich, A.F., Dickey, B.F., Lin, W., Adachi, R., and Südhof, T.C. (2006). Synaptotagmin-2 is essential for survival

and contributes to Ca2+ triggering of neurotransmitter release in central and neuromuscular synapses. J. Neurosci. *26*, 13493–13504.

Patel, M.R., Lehrman, E.K., Poon, V.Y., Crump, J.G., Zhen, M., Bargmann, C.I., and Shen, K. (2006). Hierarchical assembly of presynaptic components in defined C. elegans synapses. Nat. Neurosci. *9*, 1488–1498.

Pobbati, A.V., Razeto, A., Boddener, M., Becker, S., and Fasshauer, D. (2004). Structural basis for the inhibitory role of tomosyn in exocytosis. J. Biol. Chem. *279*, 47192–47200.

Rhee, J.S., Betz, A., Pyott, S., Reim, K., Varoqueaux, F., Augustin, I., Hesse, D., Südhof, T.C., Takahashi, M., Rosenmund, C., and Brose, N. (2002). Beta phorbol ester- and diacylglycerol-induced augmentation of transmitter release is mediated by Munc13s and not by PKCs. Cell *108*, 121–133.

Richmond, J.E., Davis, W.S., and Jorgensen, E.M. (1999). UNC-13 is required for synaptic vesicle fusion in C. elegans. Nat. Neurosci. *2*, 959–964.

Rosahl, T.W., Spillane, D., Missler, M., Herz, J., Selig, D.K., Wolff, J.R., Hammer, R.E., Malenka, R.C., and Südhof, T.C. (1995). Essential functions of synapsins I and II in synaptic vesicle regulation. Nature *375*, 488–493.

Rosenmund, C., and Stevens, C.F. (1996). Definition of the readily releasable pool of vesicles at hippocampal synapses. Neuron *16*, 1197–1207.

Rosenmund, C., Sigler, A., Augustin, I., Reim, K., Brose, N., and Rhee, J.S. (2002). Differential control of vesicle priming and short-term plasticity by Munc13 isoforms. Neuron *33*, 411–424.

Sakisaka, T., Yamamoto, Y., Mochida, S., Nakamura, M., Nishikawa, K., Ishizaki, H., Okamoto-Tanaka, M., Miyoshi, J., Fujiyoshi, Y., Manabe, T., and Takai, Y. (2008). Dual inhibition of SNARE complex formation by tomosyn ensures controlled neurotransmitter release. J. Cell Biol. *183*, 323–337.

Schoch, S., and Gundelfinger, E.D. (2006). Molecular organization of the presynaptic active zone. Cell Tissue Res. *326*, 379–391.

Schoch, S., Deak, F., Konigstorfer, A., Mozhayeva, M., Sara, Y., Südhof, T.C., and Kavalali, E.T. (2001). SNARE function analyzed in synaptobrevin/VAMP knockout mice. Science *294*, 1117–1122.

Schoch, S., Castillo, P.E., Jo, T., Mukherjee, K., Geppert, M., Wang, Y., Schmitz, F., Malenka, R.C., and Südhof, T.C. (2002). RIM1alpha forms a protein scaffold for regulating neurotransmitter release at the active zone. Nature *415*, 321–326.

Serra-Pages, C., Medley, Q.G., Tang, M., Hart, A., and Streuli, M. (1998). Liprins, a family of LAR transmembrane protein-tyrosine phosphatase-interacting proteins. J. Biol. Chem. *273*, 15611–15620.

Siksou, L., Rostaing, P., Lechaire, J.P., Boudier, T., Ohtsuka, T., Fejtova, A., Kao, H.T., Greengard, P., Gundelfinger, E.D., Triller, A., and Marty, S. (2007). Three-dimensional architecture of presynaptic terminal cytomatrix. J. Neurosci. *27*, 6868–6877.

Südhof, T.C. (2004). The synaptic vesicle cycle. Annu. Rev. Neurosci. *27*, 509–547.

Takao-Rikitsu, E., Mochida, S., Inoue, E., Deguchi-Tawarada, M., Inoue, M., Ohtsuka, T., and Takai, Y. (2004). Physical and functional interaction of the active zone proteins, CAST, RIM1, and Bassoon, in neurotransmitter release. J. Cell Biol. *164*, 301–311.

Varoqueaux, F., Sigler, A., Rhee, J.S., Brose, N., Enk, C., Reim, K., and Rosenmund, C. (2002). Total arrest of spontaneous and evoked synaptic transmission but normal synaptogenesis in the absence of Munc13-mediated vesicle priming. Proc. Natl. Acad. Sci. USA *99*, 9037–9042.

Wagh, D.A., Rasse, T.M., Asan, E., Hofbauer, A., Schwenkert, I., Durrbeck, H., Buchner, S., Dabauvalle, M.C., Schmidt, M., Qin, G., et al. (2006). Bruchpilot, a protein with homology to ELKS/CAST, is required for structural integrity and function of synaptic active zones in Drosophila. Neuron *49*, 833–844.

Wang, Y., Liu, X., Biederer, T., and Südhof, T.C. (2002). A family of RIM-binding proteins regulated by alternative splicing: Implications for the genesis of synaptic active zones. Proc. Natl. Acad. Sci. USA *99*, 14464–14469.

Zhen, M., and Jin, Y. (1999). The liprin protein SYD-2 regulates the differentiation of presynaptic termini in C. elegans. Nature *401*, 371–375.